A new energy-based ground motion selection and modification method limiting the dynamic response dispersion and preserving the median demand

(Article begins on next page)

28 April 2024

A NEW ENERGY-BASED GROUND MOTION SELECTION AND MODIFICATION METHOD LIMITING THE DYNAMIC RESPONSE DISPERSION AND PRESERVING THE MEDIAN DEMAND

S. Marasco[1], G.P. Cimellaro[2]

ABSTRACT

A novel ground motion selection and modifications method to perform response history analysis of structures is presented in this paper. Currently, the accessibility of ground motion information permits the analysis of structures using real ground motion data. Predicting the dynamic behavior of structures is a primary objective; therefore, the selection of a set of ground motions that shows a reasonable variability of the structural response and accuracy in preserving the median demand is a challenging task. The new selection and scaling procedure emerges from comparing a set of horizontal ground motions at various ranges of frequency. In this study, the Conditional Mean Spectrum and the Design Response Spectrum are used as target spectra, and the records that give an applicable and compelling contribution to the hazard are considered. It is possible to obtain a set of ground motions with similar seismic severity by matching the target spectrum at the period of interest T_{ref}, where the scaled spectrum should have an equivalent Housner intensity in the period range $0.2T_{ref}$-$2T_{ref}$. The horizontal components for every band of frequency is obtained using a specific index that depends on the energy-frequency trend's shape as well as on its scattering degree around the mean value. This allows obtaining a set of spectrum-compatible records with almost identical severity and low dispersion of the structural response parameters. The methodology has been tested showing a significant effectiveness in terms of low variability of parameters and accuracy in preserving the median demand for a given hazard scenario.

1   INTRODUCTION

The main goal of performance-based seismic design is to predict the seismic response of structures. This is achieved using different existing Finite Element Method (FEM) programs that are able to perform Non-linear Response History Analyses (NRHA). In addition, the accessibility of a vast amount of real ground motion data, recorded over the past decades, contributes in successfully performing the time-history analysis. Nowadays the trend is using real ground motion records instead of the artificial accelerograms because real earthquakes are usually distortion-free and have a more realistic energy content. Generally, the target spectrum is obtained considering the seismic hazard information at the site of interest while the structural behavior is described by the structural natural period. This constitutes the foundation of the selection ground motion selection. Different procedures for Ground Motion Selection and Modification (GMSM) are suggested to reduce the dispersion in the structural response due to different earthquakes and preserve the median demand [1].

Three selection methods based on: *scenario*, *time*, and *hazard intensity* are defined by the Seismic Performance Assessment of Buildings [2]. Intensity-based GMSM methods are performed to match the intensity measure (IM) obtained from the Probabilistic Seismic Hazard Analysis (PSHA)[3]. This is performed by modifying real ground motion records. Every ground motion record is modified in such a way to match the target response spectrum. The spectral acceleration that is consistent with

---

[1] PhD Student, Department of Civil Structural & Geotechnical Engineering, Politecnico di Torino, Italy, sebastiano.marasco@polito.it

[2] Visiting Professor, Department of Civil and Environmental Engineering, University of California, Berkeley, CA, USA, gianpaolo.cimellaro@polito.it

the fundamental period of the structure (with 5% damping ratio) is the most commonly used IM parameter. In these cases, selection of records is based on the mean compatibility between the response spectrum and the target spectrum. The dispersion between the elastic and target response spectra has been taken into account by many researchers. Ambraseys et al. [4] suggested the verification of the spectral compatibility of a certain record according to the parameter reported in Equation (0).

$$D_{ms} = \frac{1}{N} \sqrt{\sum_{i=1}^{N} \left(\frac{Sa_0(T_i)}{PGA_0} - \frac{Sa_S(T_i)}{PGA_S} \right)^2} \tag{0}$$

where N is the number of periods within the reference interval and $Sa_0(T_i)$ is the spectral acceleration of the record at period T_i. $Sa_s(T_i)$ is the target spectral acceleration at the same period value, and PGA_0 and PGA_s are the peak ground acceleration of the considered record and of the target, respectively. In addition, Iervolino et al. [5] reported the mean deviation of the record's spectra with respect to the target spectrum in a specific period range (Equation (0)).

$$D_i = \sqrt{\frac{1}{N} \sum_{i=1}^{N} \left(\frac{Sa_j(T_i) - Sa_S(T_i)}{Sa_S(T_i)} \right)^2} \tag{0}$$

Here, the PGA value is not taken as a normalizing factor and $Sa_j(T_i)$ represents the spectral acceleration of the jth record at period T_i. The methodology proposed by Iervolino et al. [5] has been implemented in the REXEL software.

Bradley [6] proposed a ground motion selection procedure based on the generalized conditional intensity measure (GCIM) approach. The method is applied by using random realizations from the conditional multivariate distribution of intensity measures derived by the GCIM approach. This method allows to select natural, synthetic and simulated motions considering any number of IM assumed as important parameters in the dynamic structural response assessment.

On the other hand, the scenario-based assessment is performed considering the source-to-site distance, faulting system, soil category, and earthquake magnitude. Shome et al. [7] picked real accelerograms built upon the basis of four different magnitude-distance pairs (*M-R*), restricting the variation in the target values. Previous research has failed to come up with an efficient M-R based procedure for the structural dynamic response. Baker and Cornell confirmed [8] that the source-to-site distance is not statistically of great importance to the response of the structure. On the other hand, they reported that earthquake magnitude is a key factor. It is worth noting that if soil response or liquefaction analyses are to be performed, the soil profile characteristics must be integrated in the selection process. In these cases, the cyclic action of the motion influences the response of the soil. Thus, the aim is to achieve a set of accelerograms that do not have significant gaps in the Fourier Amplitude Spectrum (FAS) and in the duration. The selection procedure has to be carried out considering a full classification of the site in terms of shear wave velocity at the uppermost 30 m ($V_{S,30}$) and the magnitude that influences the duration of the ground motion.

The performance of a structure subjected to a dynamic excitation is strongly dependent on the frequency content of the input. Thus, the comparison of the energy content of the motions with the target energy content represents a new approach focused on the minimization of the structural response dispersion and accuracy in the mean dynamic response prediction. In addition, the ground motion scaling is performed to have similar severity that produces a comparable structural damage. In the context of performance-based design, the proposed GMSM methodology ensures a suitable approach to assess the dynamic response of a structural and geotechnical system.

Further details on the proposed methods are given in section 2 including the novelty and benefits of the method. A case study illustrating application of the method for a steel building is presented in paragraph 3. In addition, a second case study is presented in paragraph 4. In the latter, a reinforced concrete pier bridge is investigated, using the software OPENSIGNAL 4.1 [9] for the GMSM procedure.

2 DESCRIPTION OF THE METHOD

A novel GMSM procedure for minimizing the dispersion of the Engineering Demand Parameters (EDP) and enhancing the accuracy in the prediction of dynamic structural response is proposed. The estimation in the response of the structural system subjected to a seismic action is affected by the uncertainty in the ground motion selection and in the dynamic response of the structure. The uncertainty in the ground motion selection for a given site may be reduced considering a range of magnitude and source-to-site distance (such as source-to-site distance). Moreover, the variability of the waveform characteristics of the input affects the estimation of the fragility functions. The proposed method allows to select ground motions having a limited variance of waveform characteristics such as peak parameters and input energy content parameters. Reducing the record-to-record variability enchances the estimation of the dynamic structural response and its fragility [10]. In fact, the seismic response dispersion, and its accuracy, is strongly correlated to parameters describing the seismic input. The natural records are selected in order to have a similar intensity measure and a low record-to-record variability. Therefore, the selected set of motions produce a structural dynamic response that reflects the median demand with a reduced dispersion.

In the structural assessment process, the increase in accuracy leads to a better estimation of the aftermath consequences.

2.1 Selection of the target spectrum

Finding the target spectrum is the first step in the selection procedure. One target spectrum that is widely used is the Uniform Hazard Spectrum (UHS). This comes from the PSHA [2] and defines the locus of spectral acceleration at each period having a given exceedance probability. Ground motions with different magnitudes and source-to-site distance values contribute to the total hazard. One of the observed key differences is that near-source earthquakes control the high frequency part of the UHS, while distant earthquakes influence low frequency. The UHS is not representative as target spectrum for any individual seismic excitation because no single earthquake will produce a response in a wide range of frequency content. This in turn draw attention to the Conditional Mean Spectrum (CMS-ε) that is obtained conditioning on a spectral acceleration at only one period according to commonly used de-aggregation parameters M, R and ε [8][11]. The last parameter is a measure of the difference between the mean logarithmic spectral predicted demand and the logarithmic spectral acceleration of a record with a predefined attenuation model for the site of interest. Baker and Cornell [8] looked into the dynamic response of a Multi Degree Of Freedom (MDOF) system taking into account the ground motion records having a specific intensity and matching UHS and CMS-ε. The selected records that are based on the CMS-ε generated less dispersion in the dynamic response of structures.

2.2 Ground motion scaling

Typically, the spectral acceleration at reference period ($S_a(T_{ref})$) is the intensity measure parameter (IM) used in the ground motion selection approach. This measure provides information on the maximum elastic seismic action on the structure. For MDOF structural systems, the reference period T_{ref} may be taken equal to the first mode (T_1). This is because the dynamic response of the system is dominated by the first mode. In such a case when the stiffness and the mass of the structural system are non-uniformly distributed, the dynamic response is computed as a combination of the different modes. A modal participation factor with a value greater than 85% in both directions is recommended. In these cases, the reference period may be derived from weighted arithmetic mean of the periods corresponding to the investigated modes with modal participation factors (Equation (0)).

$$T_{ref,h} = \frac{\sum_{i=1}^{N} T_{i,h} \cdot |g_{i,h}|}{\sum_{i=1}^{N} |g_{i,h}|}$$ (0)

135

136 where T_i and g_i represent the ith mode's period and modal participation factor, respectively, while h
137 index is related to the horizontal motion component. The amount of the real ground motion records
138 that are freely accessible is not sufficient to have a great number of motions having identical spectral
139 acceleration at the same period. It is essential to modify the records to have multiple sets of compatible
140 ground motions. Most of the existing modification procedures are based on scaling the spectral
141 acceleration at reference period ($S_{a,i}(T_{ref})$) to the target spectral acceleration ($S_{a,TS}(T_{ref})$) (Equation (0)
142). This approach considers records resulting in the same maximum elastic seismic action on the
143 structure.

$$SF_{I,i} = \frac{S_{a,TS}(T_{ref})}{S_{a,i}(T_{ref})}$$ (0)

144

145 In the proposed methodology, each record is adjusted in two parallel ways. Equation (0) is used to
146 carry out the first modification approach, while the second modification method is based on the
147 Housner intensity of the motion within the considered range of period.
148 Housner intensity is evaluated for every record in the range $\Delta T = 0.2 \cdot T_{ref} - 2 \cdot T_{ref}$ ($IH_{,i}(\Delta T)$) which is the
149 interval period in which the mean spectrum-compatibility has to be validated. Pseudo Velocity
150 Spectrum (*PVS*) is used to calculate the target Housner intensity ($IH_{,TS}(\Delta T)$). Equation (0) shows the
151 Housner intensity-based scale factor of the ith record.

$$SF_{II,i} = \frac{I_{H,TS}(\Delta T)}{I_{H,i}(\Delta T)}$$ (0)

152

153 *2.3   Ground motion selection*

154

155 The selection method depends on the energy content of the ground motion in the different frequency
156 bands. It is well known that the energy of the periodic signal is proportional to its squared amplitude.
157 As indicated by Fourier, a generic time history can be decomposed in infinite harmonic periodic
158 functions with given amplitude (A_i) and circular frequency (ω_i). The Fourier transform provides
159 indication in the amplitude contribution for every frequency of the ground motion. The Fourier series
160 is used to calculate the trend of the squared amplitude (A_i^2) in the frequency domain. The frequency
161 domain is sampled in different bands (Δf) of 0.5 Hz. In addition, the total energy-proportional
162 coefficient is evaluated for every Δf as the summation of each contribution in the given frequency
163 band. The amplification function (*|A|*) is used to calculate the target energy content as the ratio
164 between the spectral acceleration at the period under consideration and the period corresponding to
165 $T=0$ (*PGA*). The CMS-ε for the given site has been selected as target spectrum and sampled in
166 intervals $\Delta T=0.05$ *s* and the amplification function corresponding to the generic i^{th} period is given by
167 (Figure 1.a).

$$|A_i| = \frac{S_{a,TS}(T_i)}{S_{a,TS}(T=0)} = \frac{S_{a,TS}(T_i)}{PGA_{TS}}$$ (0)

168

169 where $S_{a,TS}(T_i)$ represents the target spectral acceleration at the generic period T_i, while PGA_{TS} is the
170 target peak ground acceleration.
171 According to the definition of the amplitude function and by setting a damping ratio ξ equal to 5%,
172 the exciting target frequency ($\omega_{f,i}$) is computed (Equation (0)).

4

173

$$| A_i | = \frac{1}{\sqrt{\left(1 - \left(\frac{\omega_{f,i}}{\omega}\right)^2\right)^2 + \left(2 \cdot \xi \cdot \frac{\omega_{f,i}}{\omega}\right)^2}} \qquad (0)$$

174 Then the terms $|A_i|^2$ and $\omega_{f,i}$ are determined by repeating the same approach for each sampled period
175 (Figure 1.b). The target percentage energy content is acquired by splitting the frequency domain into
176 multiple bands of *0.5Hz* and then aggregating their contributions. For the kth frequency band, the
177 target percentage energy contribution ($E_{p,k}(TS)$) is given by Equation (0) (Figure 1.c).

178
$$E_{p,k(TS)} = \frac{\sum_{\Delta f_k = 0.5\,Hz} \left(| A_k |\right)^2}{\sum_{k=1}^{N} \left(| A_k |\right)^2} \qquad (0)$$

179 where $\sum_{k=1}^{N} \left(| A_k |\right)^2$ represents the total energy-proportional coefficient in the frequency domain that is

180 sampled in *N* total bands.

(a)   (b)   (c)
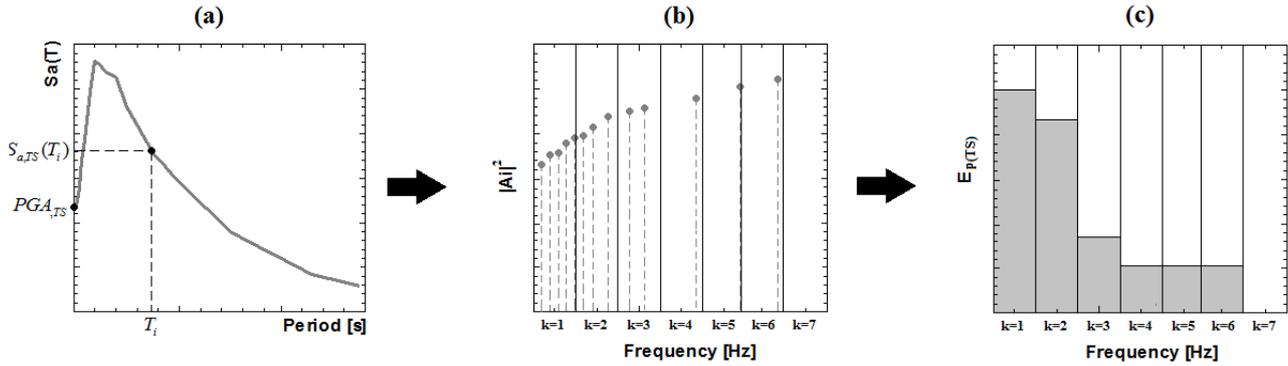
181
182 Figure 1. Scheme of the procedure used to obtain the target energy content in the discretized
183 frequency domain. (a) Discretization of the period domain, calculation of the amplification function
184 and evaluation of the associated frequencies, (b) definition of the distribution of $(|A_i|)^2 - \omega_{f,i}$ and (c)
185 target energy-proportional coefficient for each kth frequency band.

186 *2.4   Summary of the methodology*

187

188 Scaling and selection procedure is summarized in the following steps:
189 1) Set a maximum and a minimum value for the SF_I and select all the records in such a way to be
190   within the interval $SF_{I(min)}$-$SF_{I(max)}$.
191 2) A maximum absolute percentage dispersion of the PGA (σ_{PGA}) with respect to the target PGA is
192   assigned. This step allows to minimize the PGA variance of the records for a given hazard
193   scenario.
194 3) Maximum and minimum values are set for the moment magnitude and the source-to-site distance
195   according to the de-aggregation study of the site. This permits to select significant records within
196   the seismogenic characteristics of the selected site.
197 4) The Housner intensity-based scale factors are evaluated for the modified ground motion (SF_{II}).
198   Thus, only ground motions matching the target Pseudo Velocity Spectrum (PSV) in the selected
199   period range are considered.
200 5) The selection is carried out considering the ground motion having equal values for SF_I and SF_{II}.
201   Since the number of motions available in the strong motion database is reduced, a small variance
202   between the two values of the scale factors (σ_{SF}) has to be fixed. Thus, the ratio between the two
203   scale factors must be limited in the range given by Equation (0).

204
$$(1-\sigma_{SF}) \le \frac{SF_{I,i}}{SF_{II,i}} \le (1+\sigma_{SF}) \tag{0}$$

205   Generally a variance value less than 15% is suggested.

206   6) Preliminarily, only records satisfying the conditions mentioned in steps 2, 3, and 5 are selected
207   (compatible records).

208   7) Finally, only seven records have to be selected (in both horizontal directions for structural
209   analysis, and in a single horizontal direction for soil response analysis). The selection procedure
210   is performed comparing the energy content of each compatible record with the target energy
211   content. For a general compatible record, the energy trend coefficient (C_E) is computed as in
212   Equation (0).

213
$$C_E = \frac{1}{\left\{ |E_{p,k(i)} - E_{p,k(TS)}| \cdot \left[\sum_{j=1}^{20} |E_{p,k(i)} - E_{p,k(TS)}| \right] \right\}} \tag{0}$$

214   where $E_{p,k(i)}$ and $E_{p,k(TS)}$ represent the total energy percentage content for the kth frequency band of
215   the ith record and of the target, respectively. The summation in the denominator indicates the total
216   dispersion of the energy content of the ith record with respect to the target.

217   For every frequency band, all the records are arranged in a descending order of C_E values. Typically,
218   the frequency components of a seismic signal are contained between 0.1 and 10 Hz. Considering the
219   maximum frequency threshold as 10 Hz and assuming a frequency band amplitude of 0.5 Hz, the
220   total number of frequency bands to be analyzed are 20. Therefore, the summation expressed in
221   Equation (0) is performed for 20 different frequency bands.

222   As indicated by the percentage contributions of energy band content, a number n_k of records is chosen
223   for every band so as to have the greater values for the energy trend coefficient. This strategy begins
224   from Δf: 0-0.5Hz and is halted when the number $\sum_{k=1} n_k$ accomplishes a value of 7.

225   *2.5   Advantages of the methodology*

226

227   a) Spectral acceleration-based selection procedures are somehow problematic because the PGA may
228   not be close in value to the PGA derived from the hazard analysis. One reason could be the
229   inadequacy of the spectrum compatibility within the low periods range. In addition, a large
230   variance of the PGA of a records group may create high dispersion of the maximum dynamic
231   response of the structure. Nevertheless, the variation can be limited by assigning a maximum
232   absolute dispersion for the PGA (σ_{PGA}) with respect to the target.

233

234   b) The initially proposed modification method is used in other GMSM procedures. Every scaled
235   record generates identical maximum elastic actions on the structure. To avoid distortion in the
236   frequency and energy content, the maximum and minimum scale factor limits ($SF_{I(min)}$ and
237       $SF_{I(max)}$) have to be assigned. The ratio between the scale factor based on the reference spectral
238   acceleration and on the Housner intensity does not to exceed the value of $1 \pm \sigma_{SF}$. This is
239   equivalent to expect constant values of Housner intensity as well as to generate similar elastic
240   seismic action on structure. The Housner Intensity correlates the severity of seismic events with
241   building structural damage. Thus, each adjusted record generates an approximately similar
242   structural damage. Furthermore, the equal Housner intensity allows controlling the average trend
243   of the *PSV* and then the acceleration response spectrum for every record. The selected records
244   have the maximum energy content representativeness with the target energy distribution.
245   Furthermore, the consistency of the *PGAs* with the relative hazard value makes the peak amplitude
246   of the records quite similar. Therefore, the proposed selection procedure has the potential to

247   influence and control the energy input of the structure. This in turns provides a group of motions
248   with a contained variance in the seismic energy content (e.g. Arias Intensity).
249

250 c) Tso et al. [12] claimed that the energy and frequency content of a ground motion are associated
251   with the ratio between the peak value of acceleration and peak value of velocity (*AV* ratio). After
252   analyzing 45 records, three classes of *AV* ratio were identified (low, intermediate, and high).
253   Records of a given group have shown a similar trend in terms of energetic content in the frequency
254   domain. Since the records selected have moderate variability of energetic contents in frequency
255   domain, each of them assume a small variability of *AV* ratio.
256

257 d) Structural damage caused by seismic activities is proportional to the number (*n*) and amplitude
258   (*m*) of the plastic load-unload cycles. Manfredi and Cosenza [13] proposed an index for structural
259   damage (I_D) through the Arias intensity (I_A), *PGA*, and *AV* ratio (Equation (0)).

$$I_D = \frac{2 \cdot g}{\pi} \cdot \frac{I_A}{PGA^2} AV \qquad (0)$$

261   Equation (0) reports the ground motion hysteretic energy demand (E_H) as damage severity
262   parameter.

$$E_{h,d} = F_y \cdot \left(\Delta u_{\max} - \Delta u_y\right) \cdot \left[1 + m \cdot (n-1)\right] \qquad (0)$$

264   where *m* and *n* are directly proportional to I_D. The parameters F_y and Δu_y identify the yielding
265   action and displacement, respectively. These terms are related to the structure and they are
266   independent of any external agents, while Δu_{max} is the maximum dynamic response in terms of
267   displacements.
268   The low variability of the *PGA*, *AV* ratio, damage severity (expressed by means of the hysteretic
269   energy demand E_H), and Arias intensity (I_A) prompts a controlled dynamic response of the
270   structure (Δu_{max}). The dynamic response of multi-story buildings can be alternatively expressed
271   as the sum of drift contribution at each story ($\sum_i \Delta u_{\max,i}$). The proposed GMSM procedure ensures

272   a maximum control over the story drift, obtaining low dispersion among the seven selected
273   records and an accurate expected response for a given IM, as indicated in Equation (0).

274   3   CASE STUDY 1

275 *3.1   Description of the structure and structural analysis*
276

277 The case study is a five-story steel hospital in the city of Oakland, California, US (Lat: 37.7792,
278 Long: -122.1620). Non-linear dynamic analyses have been performed through the structure. The
279 lateral resisting system is a dual system (moment resisting frames and braces in both directions).
280 Beams and columns have H sections, while hollowed structural section (HSS) have been assigned to
281 the braces. The software Sap2000 [14] has been used to build the FEM model of the studied structure
282 (Figure 2).
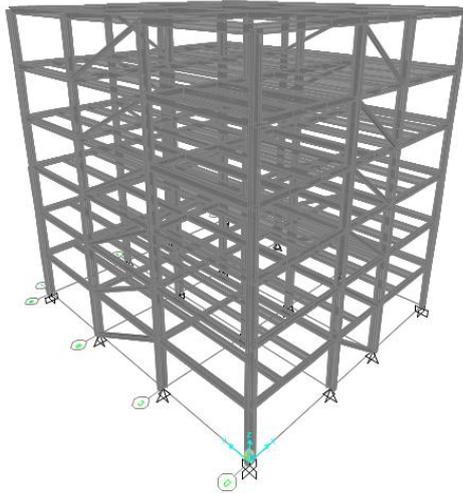
Figure 2. FEM extruded model of the case study building.

Concentrated plasticity model (FEMA 356 type P-M2-M3 for columns and M2-M3 for beams) has been chosen to account for the nonlinearity in the structural components. As for the bracing system, axial hinges have been allocated. A 3% damping ratio has been assigned to the frames according to Rayleigh formulation. Nonlinear direct integration has been used to perform the analysis. The analysis has been performed taking into consideration the P-Δ effects and applying the horizontal acceleration time histories in the two principal plan directions of the building model.

3.2   Ground motion selection and modification

Seven hazard levels (HL) have been analyzed (i.e., 75%, 60%, 50%, 20%, 10%, 5% and 2% of exceedance probability in 100 years). The mean value of the epicenter distance (R_{mean}), the logarithmic spectral offset at reference period ($\varepsilon(T_{ref})$), and the moment magnitude ($M_{W,mean}$), have been computed according to Boore-Atkinson attenuation model [15]. Further detail on the data can be found in the interactive de-aggregation of USGS (http://geohazards.usgs.gov/deaggint/2008/) [16]. The shear wave velocity at the uppermost 30 m has been assumed equal to 736 m/s according to the Global Vs30 Map Server (http://earthquake.usgs.gov/hazards/apps/vs30/) [16]. The Conditional Mean Spectrum acquired from the de-aggregation study (CMS-ε) has been taken as the target spectrum [17][1] and the model of Baker and Jayaram [18] has been considered as correlation model. OPENSIGNAL 4.1 software [9] has been used to define CMS-ε for each HL. Table 1 displays the values of the IM parameters and *PGA* for each HL.

Table 1. Spectral acceleration at first-mode period and PGA for each HL.

HL	75%	60%	50%	20%	10%	5%	2%
Sa(T$_{ref}$) [g]	0.12	0.16	0.20	0.41	0.58	0.76	0.98
PGA [g]	0.17	0.20	0.24	0.38	0.47	0.54	0.62

The first elastic mode of the building is approximately 1 sec. The related target spectral acceleration is considered as the IM parameter. Since the structure is regular in plan and elevation, the first period of the building has been assumed as the reference period (T_{ref}). Seven groups of acceleration records have been selected for each direction and for each HL according to the proposed GMSM procedure.

A comparison between the target spectrum and the mean spectrum for HL of 2% and 10% in 100 years is depicted in Figure 3. The mean spectrum has been obtained as the average of the seven groups of spectra also reported in Figure 3. The mean spectrum-compatibility is satisfied into the reference range of period.
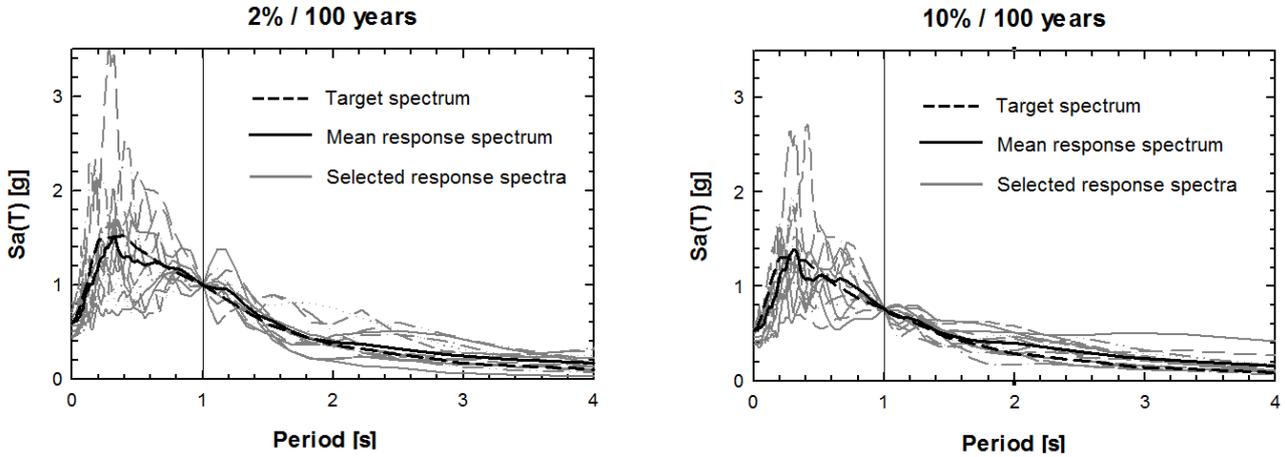
Figure 3. Spectrum-compatibility for 2% and 10% of exceedance probability in 100 years.

The spectrum-compatibility criterion is well respected especially for the periods that are close to the conditioning period.

3.3   Analysis of the results and comparison with other GMSM methods

The selected records are the input data of the non-linear analysis. A common approach is to correlate the performance of the structure to the maximum inter-story drifts that are capable of providing information about the damage state of the elements. Figure 4 indicates the response of the structure in terms of maximum drift ratio as EDP values. The response is shown as a function of the spectral acceleration at the first period of the structure (IM). The lognormal probability density distribution of the structural response has been defined by performing simple statistical analyses. This has been conducted by comparing the statistical results in terms of mean (θ) and standard deviation (β) (Figure 4).

9
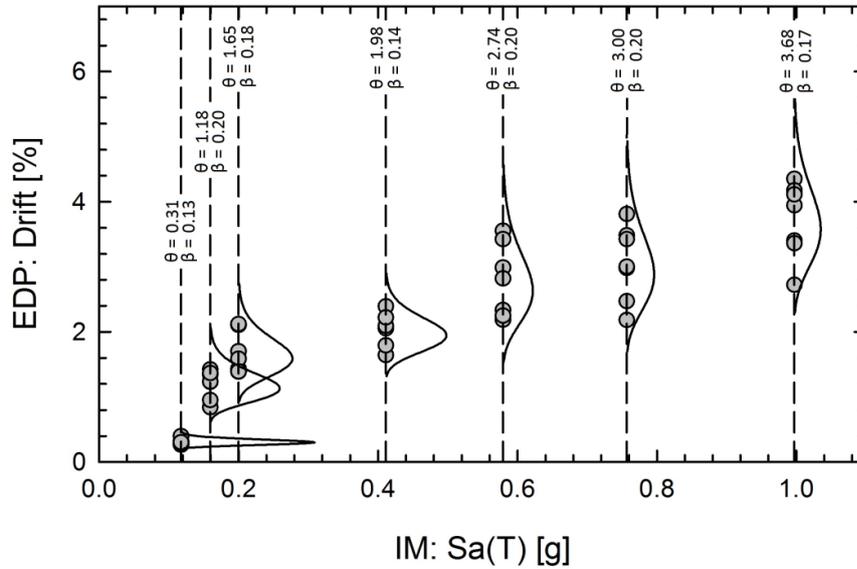
Figure 4. Maximum inter-story drift for each IM and statistical analysis of the results.

For the same structure, the selection procedure has been performed according to the spectrum-compatibility methods proposed by Ambraseys et al. [4] and Iervolino et al. [5]. The spectral acceleration at reference period of the structure has been used as IM and the same seven HLs have been assumed. In order to consistently compare the results, the same ground motion database and range of scale factors have been considered in the selection procedure. For each HL, the records selected using REXEL [5], Ambraseys, and energy-based method have been compared in terms of main ground motion characteristics (PGA, AV ratio, Arias intensity (I_A), and structural damage index (I_D)). Considering the ground motion parameters normally distributed, the mean and standard deviation values have been calculated and compared for HL having exceedance probability greater or equal than 50% in 100 years (Figure 5).
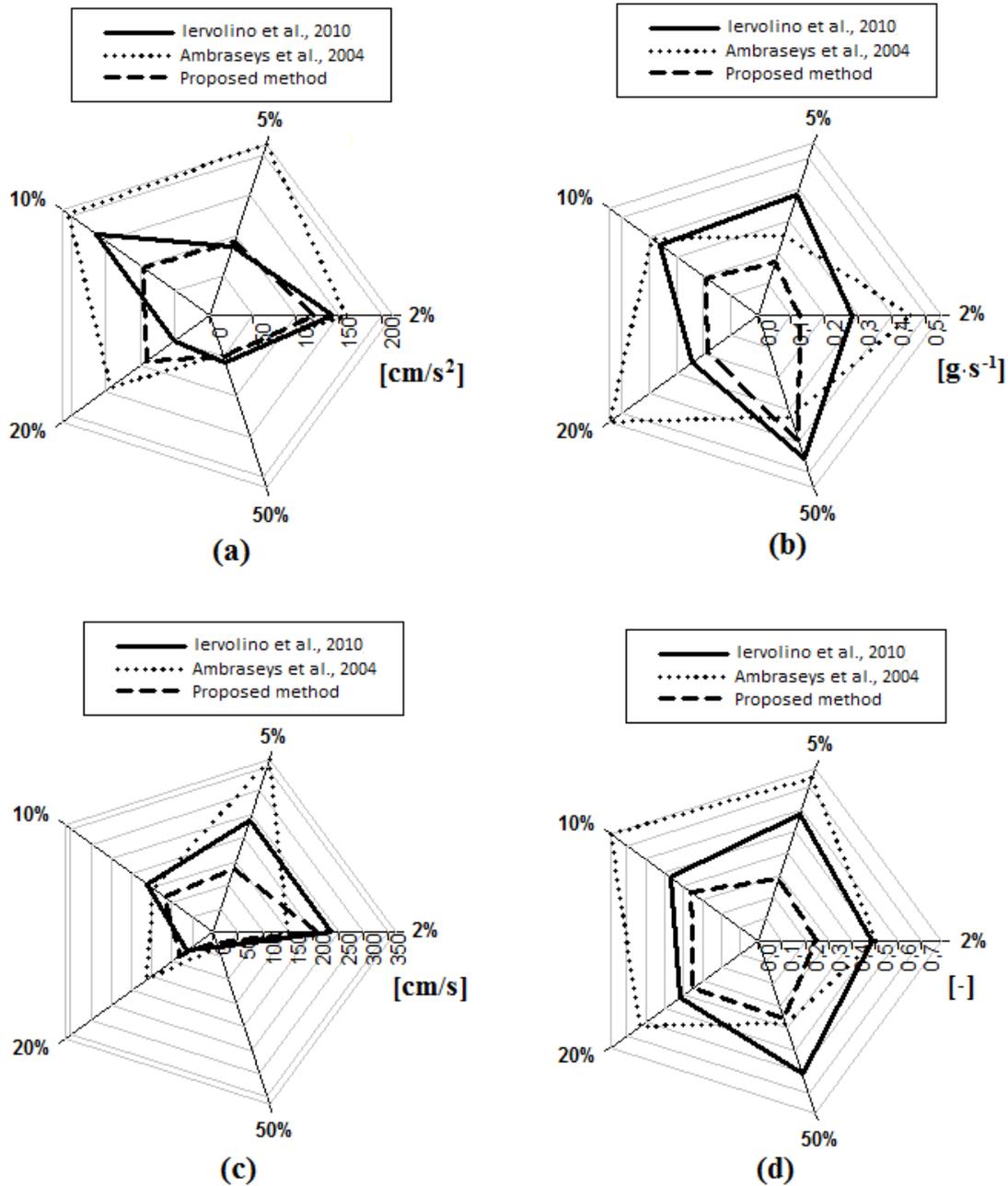
Figure 5. Comparison of the standard deviation of PGA (a), AV ratio (b), I_A (c), and I_D (d) obtained through Iervolino et al., 2010 [5], Ambraseys et al., 2004 [4] and the proposed method.

The standard deviation of the waveform characteristics gives information about the dispersion of these parameters for a given HL (record-to-record variability). The waveform parameters of the ground motions selected with the proposed method assume limited values of standard deviation compared with the other two considered methods, especially for the structural damage index (I_D). This is reflected on the structural response by limiting the dispersion of the EDP for a given hazard scenario.

The records selected through the Ambraseys and Iervolino methods have been used as seismic input in the nonlinear dynamic analyses. The results in terms of logarithmic dispersion of maximum inter-story drifts (β) and median maximum inter-story drifts are compared for each HL (Figure 6).

11

356
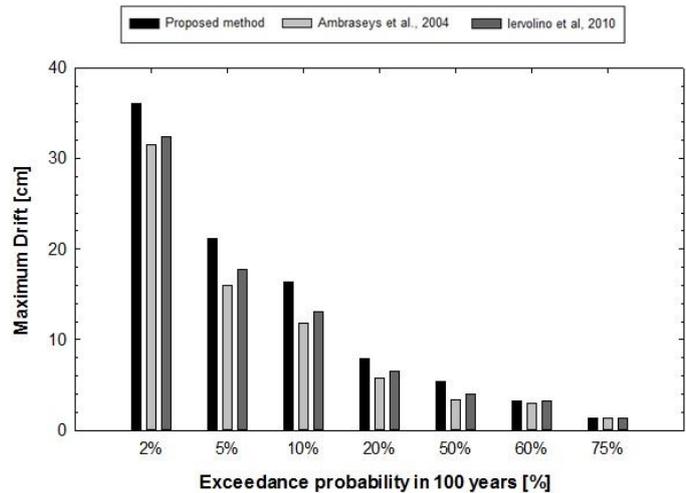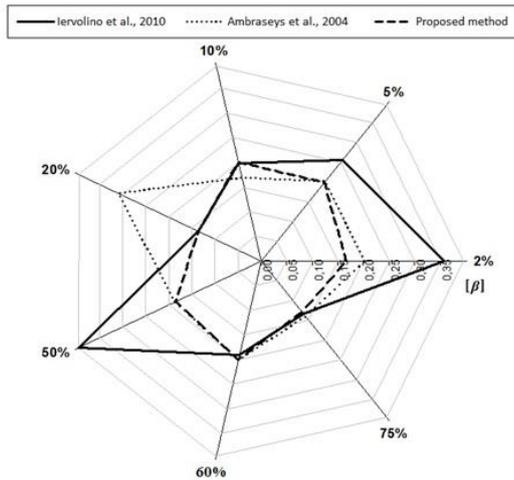
Figure 6. Comparison of the logarithmic dispersion of maximum inter-story drifts and median maximum inter-story drifts obtained through Iervolino et al., 2010 [5], Ambraseys et al., 2004 [4] and the proposed method.

The proposed method shows a low and uniform dispersion of the EDPs for each HL ($\beta \leq 0.20$) while the other two approaches present high dispersion values in some HLs.

According to the definition of Damage States (FEMA 351) [20], the related maximum inter-story drifts have been derived for each HL (expected median drifts). Moreover, the ratio between the expected median drift and the median drift demand obtained from the time history analyses has been evaluated for each HL (median drift ratio). This procedure has been carried out for the ground motions selected according to Iervolino, Ambraseys and the proposed method. **Errore. L'origine riferimento non è stata trovata.**Figure 7 depicts a comparison of the median drift ratio among the three GMSM methods.

369
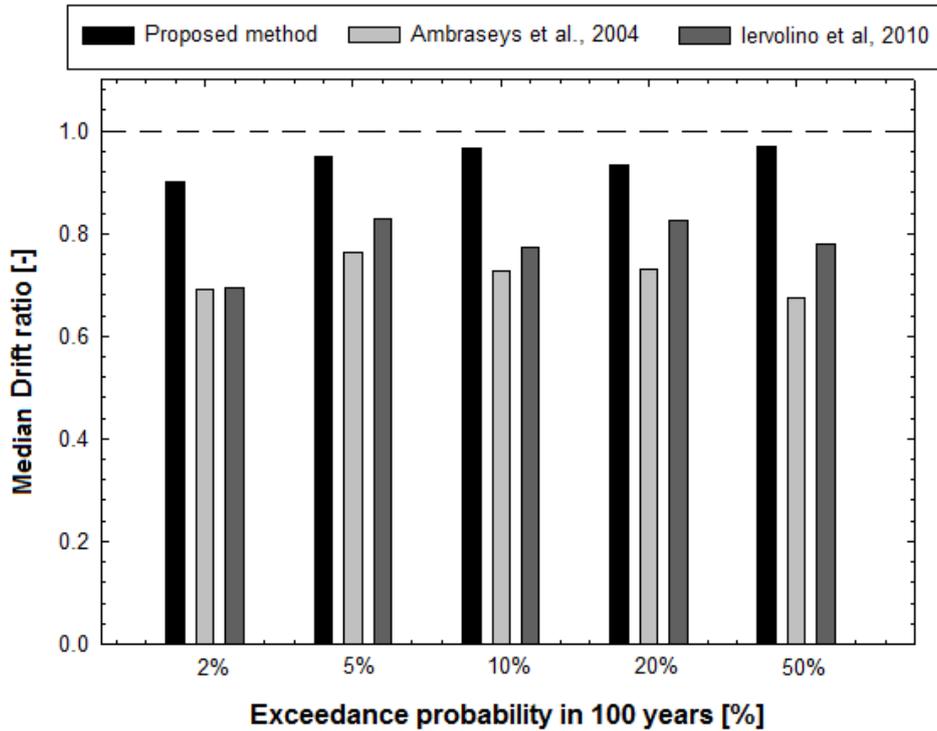
Figure 7. Comparison of the median drift ratio obtained through Iervolino et al., 2010 [5], Ambraseys et al., 2004 [4] and the proposed method..

The full accuracy with the median drift demand for a given hazard scenario is achieved when the median drift ratio is equal to one. The median drift ratio resulting from the proposed method is the closest to the unit value for each HL. Thus, the proposed method shows an adequate accuracy in preserving the median drift demand for a given hazard scenario, especially for high HLs. The fragility functions for structural systems are statistical distributions, taking a form of lognormal cumulative distribution functions, used to indicate the probability that a component, element, or system will be damaged as a function of a given EDP. According to FEMA 351 [20], the extensive and complete Damage State (DS) have been identified for the steel building depending on the maximum story drift ratio. For each DS, only the drift ratios that do not exceed the associated maximum limit have been considered and the related mean and standard deviation have been calculated. These statistical parameters have been used to derive the lognormal cumulative distribution function that represents the probability to exceed a certain level of damage on the considered structure. Figure 8 shows a comparison in terms of fragility functions obtained from the three different GMSM methods.

13
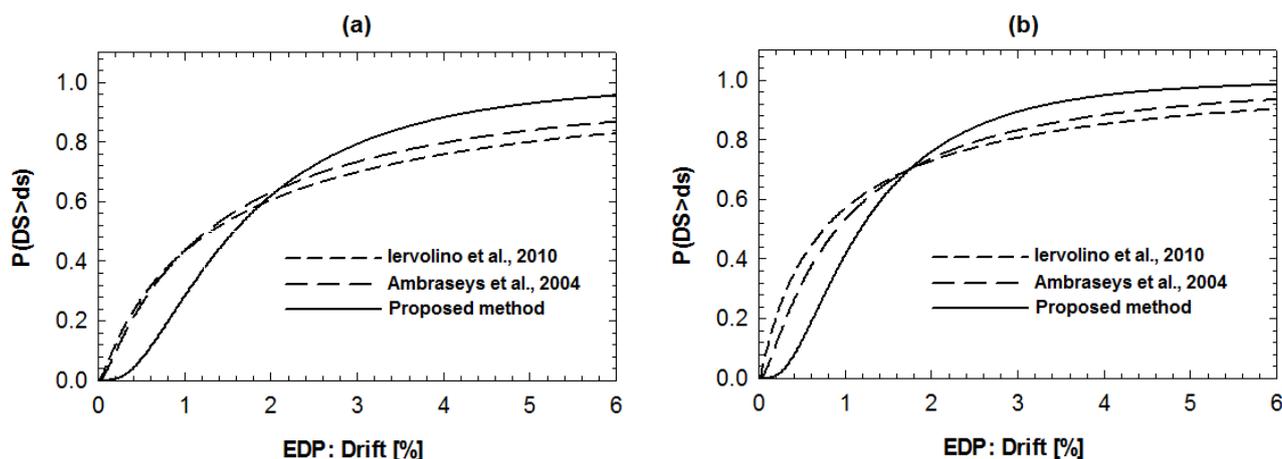
Figure 8. Comparison of the fragility curves obtained through Iervolino et al., 2010 [5], Ambraseys et al., 2004 [4] and the proposed method for extensive (a), and complete damage state (b).

Since the mean value and the dispersion of structural response influence the estimation of the fragility curves, this comparison is of high importance. The fragility curves' dispersions obtained through Iervolino and Ambraseys are greater than the dispersion derived from the proposed method. Moreover, the mean probability to exceed a certain damage state is about similar for the fragility functions resulting from the selection method proposed by Iervolino and Ambraseys. Figure 8 shows a difference in terms of mean probability to exceed complete and extensive damage states between the proposed method and the Iervolino and Ambraseys methods. This is also reflected in the comparison presented in Figure 7.

4   CASE STUDY 2

4.1   Description of the structure and structural analysis

An ordinary reinforced concrete girder bride located in the city of Savoca, Italy (Lat: 37.9558, Long: 15.3397) has been investigated. The bridge is composed of four spans with the same length. The three internal piers present a full circular cross section with symmetric reinforcement. Each pier has a total length of 23 m and rests on a circular shaft foundation that is 10.00 m high and 8.00 m in diameter. The foundation soil is a normally consolidated sand with an angle of internal friction of 30° and specific weight equal to 20 kN/m^3. The static scheme of the bridge is showed in Figure 9.
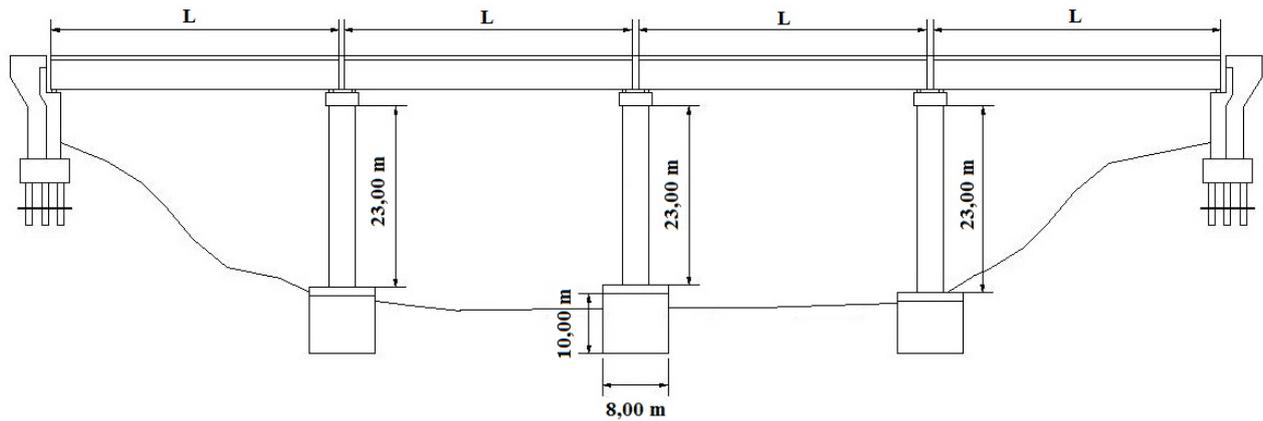
Figure 9. Static scheme of the case study bridge.

409 The design of the piers has been carried out according to European standards [21][22] while the shaft
410 foundation has been designed and verified according to the Jamiolkowski method [23]. The horizontal
411 soil-structure interaction has been taken into account by modeling the non-linear behavior of the soil
412 and considering a uniform foundation scouring of 1.00 m. According to Boulanger et al [24] and
413 Gerolymus and Gazetas [25] the soil is modeled through macro-elements composed by linear and
414 non-linear elements in series. For the case study, a plastic element and a viscous-elastic element
415 (dashpot-spring model) have been used in series to simulate the soil behavior. The software Sap2000
416 [14] has been used to model the pier and shaft foundation (model created by Rizzo A.). For the
417 horizontal soil-structure interaction, the *Non-linear-Link* element based on the Wen plastic model has
418 been considered while elastic behavior has been taken into account through the *Linear-Link* element.
419 The force-deformation relationship used to set the non-linear link element has been chosen according
420 to soil characteristic at different depth. The stiffness of the linear link elements has been assessed
421 based on the soil characteristics and assuming for each element a given interaction surface. The
422 vertical soil-structure interaction has been modeled with one *Linear-Link* element connected to the
423 bottom part of the shaft foundation. Figure 10.a depicts an extruded view of the pier connected to the
424 shaft foundation while the associated FEM model is shown in Figure 10.b. In addition, the macro-
425 element model used for the soil-interaction is illustrated in Figure 10.c.

15
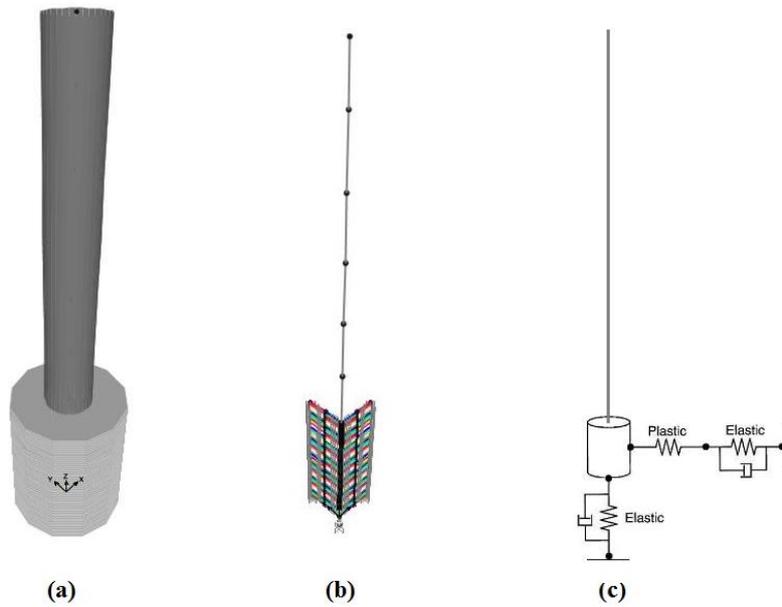
Figure 10. Extruded view of the structural model (a), FEM model (b) and macro-element model used for soil-structure interaction (c).

Concentrated plasticity model (CALTRANS type P-M2-M3) has been chosen to consider the nonlinearity in the pier. The position of plastic hinge has been supposed coincident with the pier-shaft foundation interface, while its length has been assessed according to the Italian standard [26]. The non-linear dynamic analyses have been performed taking into consideration the P-Δ effects and applying the horizontal acceleration time histories in the two principal directions of the bridge.

4.2   Ground motion selection and modification

Six HLs have been analyzed (i.e., 50%, 20%, 10%, 5%, 2% and 1% of exceedance probability in 50 years). The Italian Design Response Spectrum (DRS) has been considered as target spectrum [26]. Further details on the used hazard parameters can be found in the interactive hazard map of INGV (http://esse1-gis.mi.ingv.it/) [27]. PGA and spectral acceleration at reference period are listed in Table 2 for each HL.

Table 2. Spectral acceleration at first-mode period and PGA for each HLs.

HL	50%	20%	10%	5%	2%	1%
$Sa(T_{ref})$ [g]	0.03	0.06	0.11	0.15	0.24	0.27
PGA [g]	0.10	0.17	0.24	0.30	0.44	0.52

The fundamental period of the pier, considering the soil-structure interaction, is equal to 1.96 s. The related target spectral acceleration is considered as IM parameter. Seven groups of acceleration records have been selected for each direction and for each HL according to the proposed GMSM procedure. The software OPENSIGNAL 4.1 [9] has been used for scaling and selecting ground motions. Figure 11 illustrates the mean spectrum compatibility for the cases of 1% and 2% of exceedance probability.

16

450
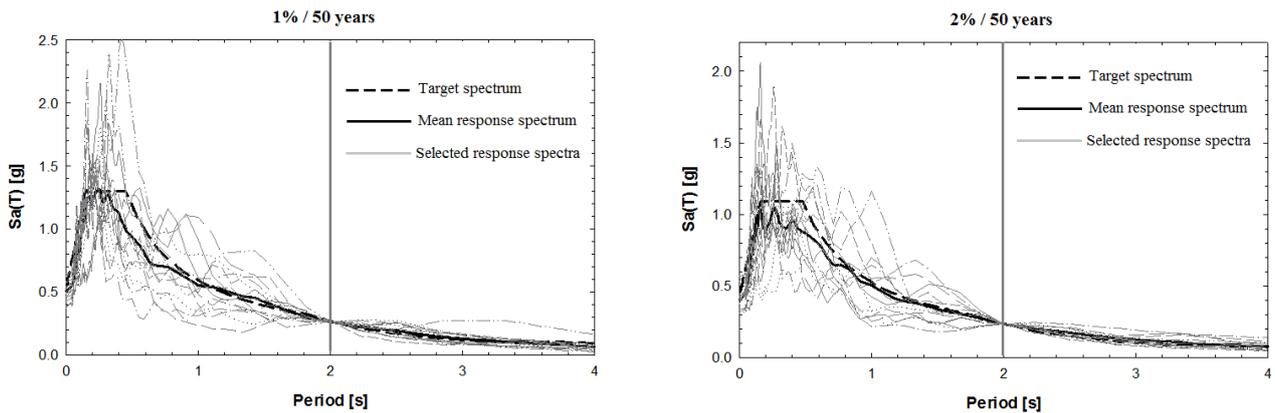
451
452   Figure 11. Spectrum-compatibility for 1% and 2% of exceedance probability in 50 years.

453   The mean spectra are close to the target spectra within the reference period range.
454

455   *4.3   Analysis of the results and comparison with other GMSM methods*
456

457   The ductility ratio (μ_d) is considered as EDP to assess the level of damage on the pier. This parameters
458   is defined as the ratio between the maximum plastic top displacement and yielding top displacement
459   of the pier. Since only the structural damage has been assessed, the soil displacement (roto-translation
460   of the shaft foundation) obtained from dynamic non-linear analyses has been removed.
461   The geometric mean of the displacements has been obtained from the non-linear analyses for all the
462   selected records, and the maximum ductility ratios have been considered as EDP. Figure 12 shows
463   the associated values depending on the spectral acceleration at the first period of the pier (IM).
464   Considering the EDPs as lognormally distributed, the mean (θ) and standard deviation (β) have been
465   calculated for each IM (Figure 12).
466
467
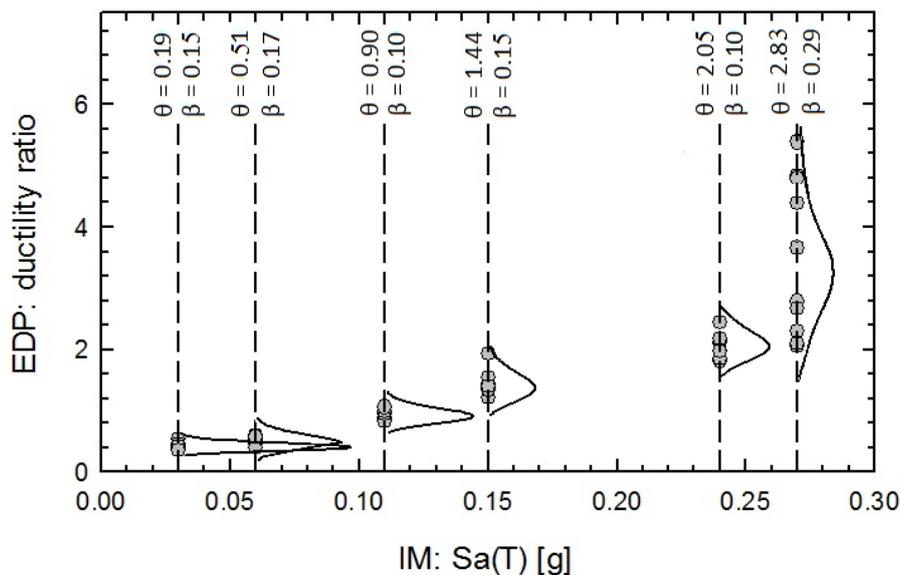
468
469   Figure 12. Maximum ductility ratio for each IM and statistical analysis of the results.

470   The dynamic post-elastic soil behavior is influenced by the number of cycles and their amplitude. For
471   high HLs, the degradation of the characteristics of the soil rapidly increases and the soil response is
472   governed by its residual parameters. As an illustrative example, the hysteretic cycles of soil at 2.00

17

473   m of depth are assessed for HL of 5 % of exceedance probability in 50 years. Figure 13 illustrates the
474   lognormal probability density function associated with the total hysteretic dissipation (E_h) and the
475   residual equivalent stiffness (k_{eq}).

(a)

(b)
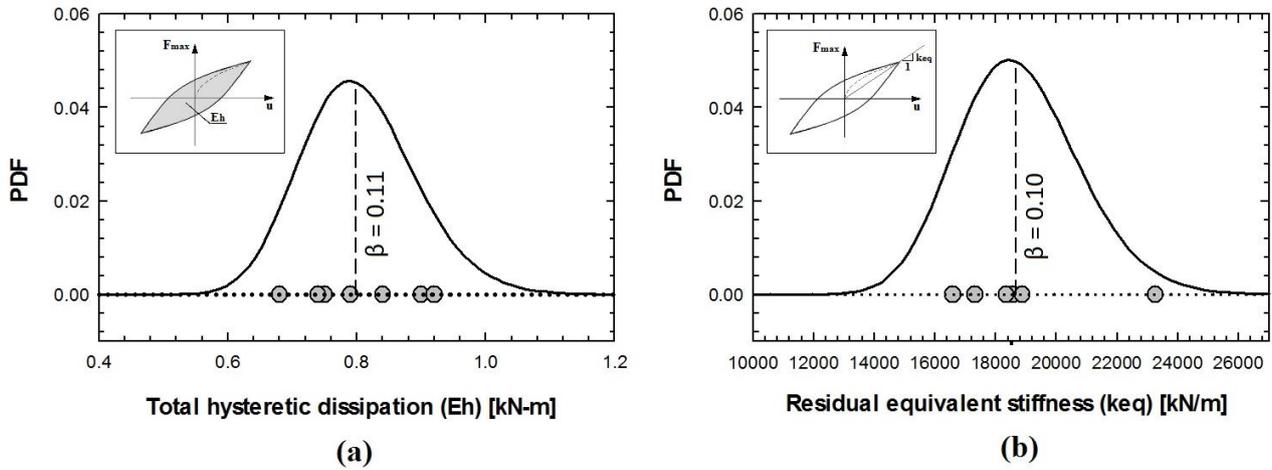
476

477   Figure 13. Total hysteretic dissipation (a) and residual equivalent stiffness (b) for soil at 2.00 m of
478   depth and 5% of exceedance probability in 50 years as HL (The standard deviations β are reported).

479   The total hysteretic dissipation and the residual equivalent stiffness have been considered as soil
480   degradation parameters. In both cases, Figure 13 shows a limited dispersion of the results obtained
481   from the dynamic non-linear analyses ($\beta \; 0.1$).
482   The dynamic response of the pier is strongly dependent on the soil behavior, which is sensitive to the
483   frequency content of the time histories. Furthermore, the maximum rotation and horizontal
484   displacement of the shaft foundation is governed by the total input energy (described by the Arias
485   intensity) and on the peak parameters. For each HL, the normal standard deviation of the *PGA* and I_A
486   resulted by the three considered GMSM methods have been compared (Figure 14).
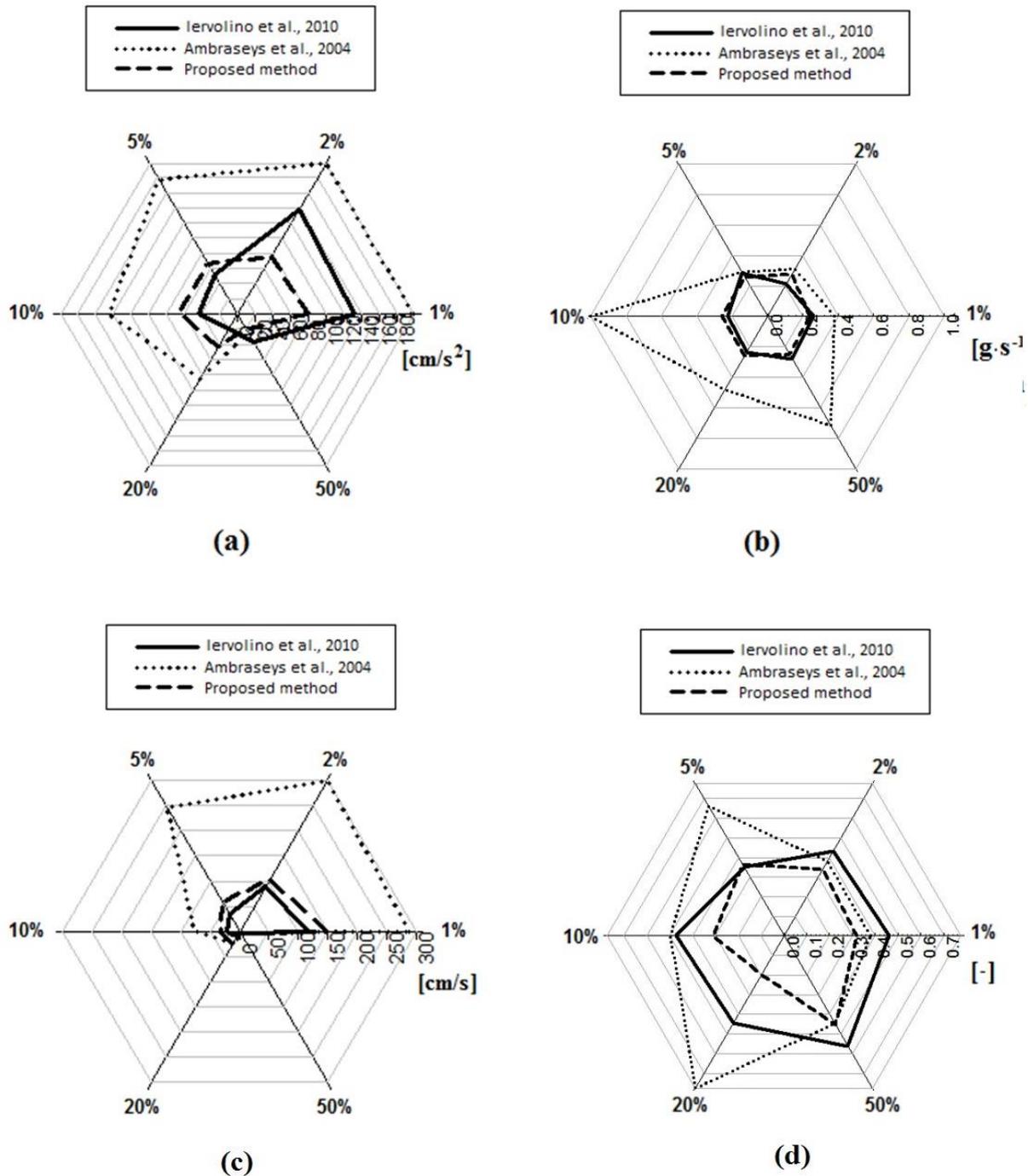
18

Figure 14. Comparison of the standard deviation of PGA (a), AV ratio (b), IA (c), and ID (d) obtained through Iervolino et al., 2010 [5], Ambraseys et al., 2004 [4] and the proposed method.

The energetic-based method allows us to obtain a bounded dispersion of the *PGA* and I_A with consequent benefits in terms of stability of the structure-soil response for a given hazard scenario. In order to evaluate the uncertainty of the dynamic response of the pier, nonlinear dynamic analyses have been performed using the set of motions resulting from Ambraseys and Iervolino method [5]. Considering the ductile ratio (IM) as lognormally distributed for a given hazard scenario, the standard deviations values and the median maximum ductility ratios have been assessed and compared (Figure 15).

19
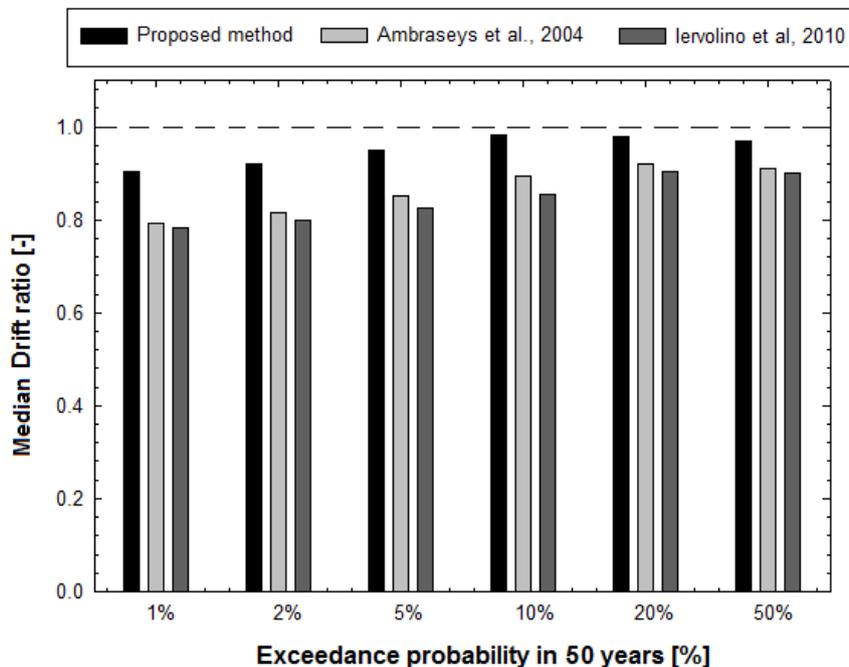
497
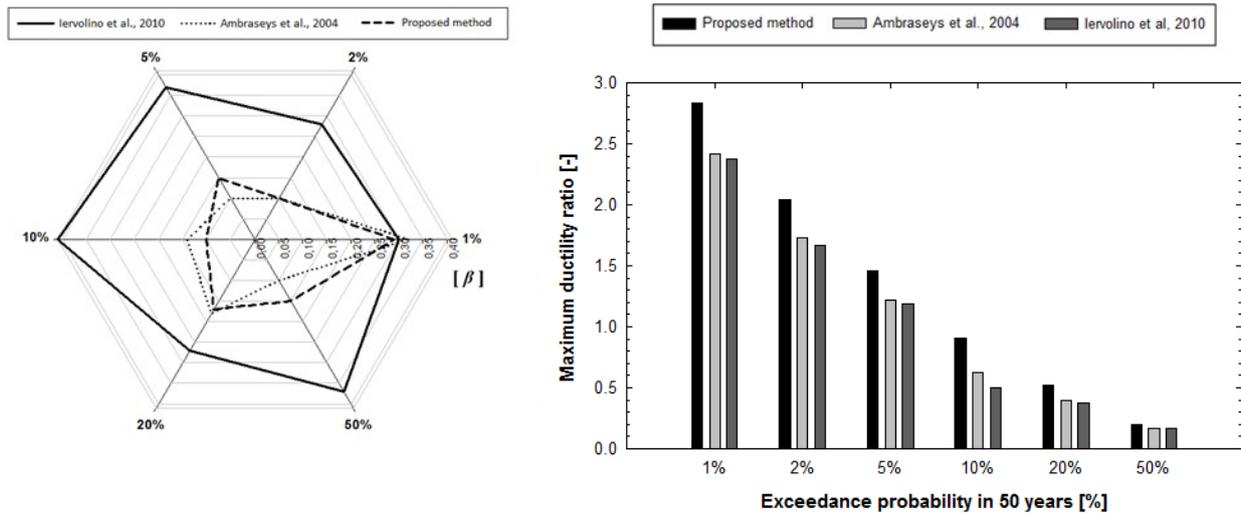
Figure 15. Comparison of the logarithmic dispersion of maximum ductility ratio and median maximum ductility ratio obtained through Iervolino et al., 2010 [5], Ambraseys et al., 2004 [4] and the proposed method.

Figure 15 shows how the structural dynamic response uncertainty is reduced using the Ambraseys and the energetic-based method. In addition, for high hazard scenario (1% of exceedance probability in 50 years) the smallest lognormal dispersion of the ductility ratio has been obtained with the proposed GMSM procedure.

A comparison in terms of median drift ratio has been carried out to verify the accuracy in preserving the median response for all hazard scenarios (Figure 16).
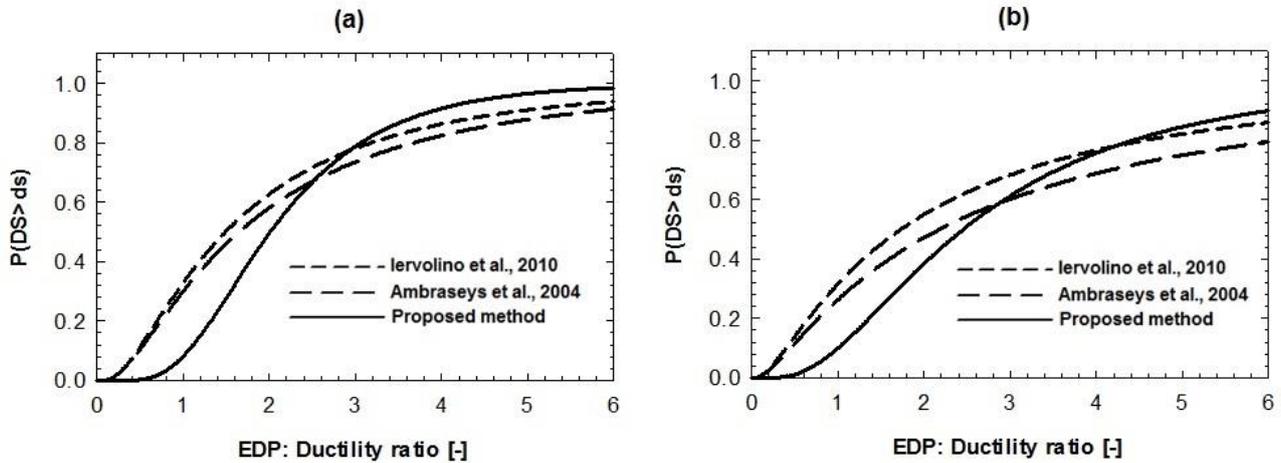

507

Figure 16. Comparison of the median drift ratio obtained through Iervolino et al., 2010 [5], Ambraseys et al., 2004 [4] and the proposed method.

According to the proposed methodology, the median drift ratio is always more representative of the median demand for the hazard scenarios. The proposed method is capable of estimating a highly representative set of EDPs for each considered hazard scenario.

20

513 The extensive and complete DS have been considered for the reinforced concrete girder bridge de-
514 pending on the maximum ductility ratio. The DS threshold values have been assumed accordingly
515 to Banerjee et al. [28] and the fragility functions have been obtained from the three differenyt
516 GMSM methods (Figure 17).

517

518 Figure 17. Comparison of the fragility curves obtained through Iervolino et al., 2010 [5], Ambraseys
519   et al., 2004 [4] and the proposed method for extensive (a), and complete damage state (b).

520 The fragility curves' dispersions obtained through Iervolino and Ambraseys are greater than the
521 dispersion derived from the proposed method. It is also possible to observe how the mean probability
522 to exceed complete and extensive damage states for the proposed method is greater than that one
523 obtained through Iervolino and Ambraseys methods. Furthermore, the mean probability to exceed
524 complete and extensive damage states obtained with the proposed method is closer to the expected
525 one. This is also reflected in the comparison shown in Figure 16.
526

527 **5 CONCLUSION**

528 Currently, the accessibility of ground motion database permits the analysis of structures using real
529 ground motion data. Predicting the dynamic behavior of structures is a primary objective; therefore,
530 the determination of a set of ground motions that shows a small variability of the structural response
531 and accuracy in preserving the median demand is the most challenging task.
532 The new GMSM methodology is based on the energy content of the records. It helps in controlling
533 the essential variables that influence the dynamic response of structures. In addition, the selected
534 records are compatible with the seismic hazard analysis at the site of interest, in terms of the spectral
535 acceleration at the period of reference and the M-R parameters. The selected group of ground motion
536 records causes an identical elastic seismic action and approximately equal plastic dissipation on the
537 structure. The ground motions records have been selected with the main goal of assessing the
538 structural response given a certain intensity level. The analysis of the numerical results has shown
539 that the selection method significantly affects the structural response estimation and the structural
540 damage prediction. The procedure proposed in this work is able to reduce the scatter of the structural
541 response parameters around the corresponding mean values and enhance the accuracy in preserving
542 the median demand. In addition, the comparisons with other methods have shown the accuracy of the
543 estimated median EDPs for every hazard scenario. The accuracy of consequence functions (i.e.,
544 casualties, repair time, repair costs, etc.) can be increased by using, in the time history analyses, set
545 of motions having low variability and being accurate with the median demand. Therefore, the new

GMSM procedure can be used to define an earthquake scenario for resilience analyses of a single building or for a group of buildings.

ACKNOWLEDGEMENTS

REFERENCES

[1] Katsanos EI, Sextos AG, Manolis, GD (2010) Selection of earthquake ground motion records: A state-of-the-art review from a structural engineering perspective. Soil Dynamics and Earthquake Engineering 30, 157–169.

[2] Applied Technology Council (2011) Draft Guidelines for Seismic Performance Assessment of Buildings. Volume 1- Methodology ATC-58-1.

[3] Cornell CA (1968) Engineering Seismic. Risk Analysis. Bulletin of the Seismological Society of America 58(5):1583-1606.

[4] Ambraseys NN, Douglas J, Rinaldis D, Berge-Thierry C, Suhadolc P, Costa G, Sigbjornsson, R, Smit P (2004) Dissemination of European strong-motion data, vol. 2, CD-ROM collection. Engineering and Physical Sciences Research Council, UK.

[5] Iervolino I, Galasso C, Cosenza E (2010) REXEL: computer aided record selection for code-based seismic structural analysis, Bull Earthquake Eng 8:339-362.

[6] Bradley BA (2010) A generalized conditional intensity measure approach and holistic ground-motion selection. Earthquake Engng. Struct. Dyn. 39: 1321–1342. doi:10.1002/eqe.995

[7] Shome N, Cornell CA, Bazzurro P, Carballo JE (1998) Earthquakes, records and nonlinear responses. Earthquake Spectra14(3):469-500.

[8] Baker J, Cornell CA (2006) Spectral shape, epsilon and record selection. Earthquake Engineering & Structural Dynamics 35, 1077-1095.

[9] Cimellaro GP, Marasco S (2015) A computer-based environment for processing and selection of seismic ground motion records OPENSIGNAL. Front. Built Environ 2015; 1:17. DOI: 10.3389/fbuil.2015.00017.

[10] Cimellaro GP, Reinhorn AM, D'Ambrisi A, De Stefano M . Fragility Analysis and Seismic Record Selection. Journal of Structural Engineering, ASCE, 2011; 137(3), 379-390.

[11] Cimellaro GP (2013) Correlation in spectral accelerations for earthquakes in Europe. Earthquake Engng. Struct. Dyn. 42(4), 623-633.

[12] Tso WK, Zhu TJ, Heidebrecht AC (1991) Engineering implication of ground motion A/V ratio. Soil Dynamics and Earthquake Engineering 11 (1992) 133-144.

[13] Manfredi G (2001) Evaluation of seismic energy demand. Earthquake Engineering & Structural Dynamics DOI: 10.1002/eqe.17.

[14] Computer and Infrastructure Inc. Sap2000, Version 17.3, Berkeley, CA.

[15] Boore DM, Atkinson GM (2008) Ground-motion prediction equations for the average horizontal component of PGA, PGV, and 5%-damped PSA at spectral periods between 0.01 s and 10.0 s. Earthquake Spectra 24(1), 2008, 99-138.

[16] USGS. Seismic Hazard Analysis tools. U.S. Geological Survey < http://earthquake.usgs.gov/hazards/designmaps/grdmotion.php>.

[17] Baker JW (2011) Conditional Mean Spectrum: Tool for Ground-Motion Selection. Journal of Structural Engineering-Asce 137, 322-331.

[18] Lin B, Haselton CB, Baker JW (2013) Conditional-spectrum-based ground motion selection. Part II: Intensity-based assessments and evaluation of alternative target spectra. Earthquake Engng. Struct. Dyn. DOI: 10.1002/eqe.2303.

[19] Baker JW, Jayaram N (2008) Correlation of spectral acceleration values from NGA ground motion models. Earthquake Spectra 24(1), 299-317.

[20] FEMA (2000) FEMA 351: Reccomended seismic evaluation and Upgrate Criteria for Existing Welded Steel Moment-Frame Buildings. FEMA 351 Federal Emergency Management Agency, Federal Emergency Management Agency, Washington D.C.

[21] EC2 (2002) Design of concrete structures. European Committee for Standardization, Bruxelles, BG.

[22] EC8 (2005) Design of structures for earthquake resistance. European Committee for Standardization, Bruxelles, BG.

[23] Jamiolkowski M (1968) Atti e rassegna tecnica della società ingegneri e architetti di Torino n° 7, 169-172 (in Italian).

[24] Boulanger RW, Curras CJ, Kutter BL, Wilson DW, Abghari A (1999) Seismic soil-pile-structure interaction experiments and analyses. Journal of geotechnical and geo-environmental engineering 750-759.

[25] Gerolymos N, Gazetas G (2005) Winkler model for lateral response of rigid caisson foundations in linear soil, Elsevier 347-361.

[26] NTC-08 (2008) Nuove Norme Tecniche per le Costruzioni (NTC08). Consiglio Superiore dei Lavori Pubblici, Ministero delle Infrastrutture, Gazzetta Ufficiale della Repubblica Italiana, n. 29 (in Italian).

[27] INGV. The National Institute of Geophysics and Vulcanology. http://www.ingv.it/en/.

[28] Banerjee S, Shinozuka M (2008) Mechanistic quantification of RC bridge damage states under earthquake through fragility analysis, Probabilistic Engineering Mechanics 23.1 (2008): 12-22.